SPARC preserves endothelial glycocalyx integrity, and protects against adverse cardiac inflammation and injury during viral myocarditis

Rienks, Marieke; Carai, Paolo; Teeffelen, Jurgen van; Eskens, Bart; Verhesen, Wouter; Hemmeryckx, Bianca; Johnson, Daniel M.; Leeuwen, Rick van; Jones, Elizabeth A.; Heymans, Stephane; Papageorgiou, Anna-Pia

DOI:
10.1016/j.matbio.2018.04.015

Document Version
Publisher's PDF, also known as Version of record

Citation for published version (Harvard):
Rienks, M, Carai, P, Teeffelen, JV, Eskens, B, Verhesen, W, Hemmeryckx, B, Johnson, DM, Leeuwen, RV, Jones, EA, Heymans, S & Papageorgiou, A-P 2018, 'SPARC preserves endothelial glycocalyx integrity, and protects against adverse cardiac inflammation and injury during viral myocarditis', *Matrix Biology*, pp. 21-34. https://doi.org/10.1016/j.matbio.2018.04.015

SPARC preserves endothelial glycocalyx integrity, and protects against adverse cardiac inflammation and injury during viral myocarditis

Marieke Rienks[a,b], Paolo Carai[b], Jurgen van Teeffelen[d], Bart Eskens[d], Wouter Verhesen[a], Bianca Hemmeryckx[c], Daniel M. Johnson[b], Rick van Leeuwen[b], Elizabeth A. Jones[c], Stephane Heymans[b,c,e,†] and Anna-Pia Papageorgiou[b,c,†]

a - Cardiovascular Department, *King's College London, United Kingdom*
b - Center for Heart Failure Research, *Cardiovascular Research Institute Maastricht, The Netherlands*
c - Molecular and Vascular Biology, *Department of Cardiovascular Sciences, KU, Leuven, Belgium*
d - Department of Physiology, *Maastricht University, The Netherlands*
e - Netherlands Heart Institute, *ICIN, Utrecht, The Netherlands*

Correspondence to Marieke Rienks: *Cardiovascular Research Institute Maastricht, Universiteitssingel 40, 6229 ER Maastricht, The Netherlands. m.rienks@maastrichtuniversity.nl.*
https://doi.org/10.1016/j.matbio.2018.04.015

Abstract

Myocardial damage as a consequence of cardiotropic viruses leads to a broad variety of clinical presentations and is still a complicated condition to diagnose and treat. Whereas the extracellular matrix protein Secreted Protein Acidic and Rich in Cysteine or SPARC has been implicated in hypertensive and ischemic heart disease by modulating collagen production and cross-linking, its role in cardiac inflammation and endothelial function is yet unknown.

Absence of SPARC in mice resulted in increased cardiac inflammation and mortality, and reduced cardiac systolic function upon coxsackievirus-B3 induced myocarditis. Intra-vital microscopic imaging of the microvasculature of the cremaster muscle combined with electron microscopic imaging of the microvasculature of the cardiac muscle uncovered the significance of SPARC in maintaining endothelial glycocalyx integrity and subsequent barrier properties to stop inflammation. Moreover, systemic administration of recombinant SPARC restored the endothelial glycocalyx and consequently reversed the increase in inflammation and mortality observed in SPARC KO mice in response to viral exposure. Reducing the glycocalyx in vivo by systemic administration of hyaluronidase, an enzyme that degrades the endothelial glycocalyx, mimicked the barrier defects found in SPARC KO mice, which could be restored by subsequent administration of recombinant SPARC.

In conclusion, the secreted glycoprotein SPARC protects against adverse cardiac inflammation and mortality by improving the glycocalyx function and resulting endothelial barrier function during viral myocarditis.

Introduction

Myocarditis is defined as inflammation of the heart muscle and can be caused by a variety of infectious and non-infectious illnesses. Amongst the infectious causes, viruses are supposedly the most frequent pathogens affecting the myocardium. The broad variety of clinical presentations, make viral myocarditis a complicated condition to diagnose and treat. Despite combining the standardized criteria for histological diagnosis of myocarditis [1] with endomyocardial biopsy [2], the true incidence is still not precisely known yet, estimating 1 to 10 cases per 100,000 persons each year.

Not only can acute viral myocarditis lead to sudden cardiac arrest [5], but it is also a major cause of congestive heart failure [6] and in some cases even requires cardiac transplantation. Responsible cardiotropic viruses, such as the entero-coxsackie B viruses, can induce this severe cardiac inflammation in susceptible patients, resulting in heart failure and possibly sudden death. This form of heart disease is

particularly devastating as it affects previously healthy young adults. In spite of our better understanding of the causative cardiotropic viruses and consecutive immunological mechanisms that contribute to the development of cardiac dysfunction [7], diagnosis and treatment for myocarditis are still poor. Elucidating the underlying mechanisms of enhanced or sustained cardiac inflammation can facilitate the development of new specific therapies for viral myocarditis.

The cardiac extracellular matrix (ECM), comprised of proteoglycans, glycoproteins and glycosaminoglycans [8], plays an important role in intercellular communication during cardiac disease [9,10]. Since inflammation and heart failure reciprocally trigger one another [11], we speculated that ECM proteins may trigger heart failure development by potentiating the immune response [12,13]. When addressing the interaction of the immune system and the ECM in cardiac disease however, the prominent vascular gatekeeper known as the endothelial glycocalyx is often overlooked. This while the endothelial glycocalyx is comprised of similar proteoglycans, glycoproteins and glycosaminoglycans to the cardiac ECM and is known to regulate inflammation, vascular permeability, coagulation and mechanotransduction [14,15]. The endothelial glycocalyx does not just infer the luminal lining of the endothelium but in fact encapsulates endothelial cells and expand towards the endothelial basement membrane [14]. Therefore, we investigated the role of the endothelial glycocalyx in regulating inflammation in viral myocarditis in this study with a specific focus on ECM protein Secreted Protein Acidic and Rich in Cysteine (SPARC).

SPARC has been shown to regulate fibroblast function in connective tissue [16–19] as well as tumour development and progression [20,21], bone homeostasis and repair [22], angiogenesis [23] and cardiac ageing [18,24,25]. Moreover, both in vitro studies and in vivo murine oncology studies have recognized the increased vascular permeability in the absence of SPARC [26,27], however the mechanisms by which SPARC may influence vascular permeability are still unclear. Where SPARC has been recognized for its fundamental roles as an adhesive component of the ECM, no attention has been given to the extracellular lining of the endothelium as a possible immune-regulating structure housing SPARC [14]. As the expression of SPARC is low during normal post-natal life but dramatically

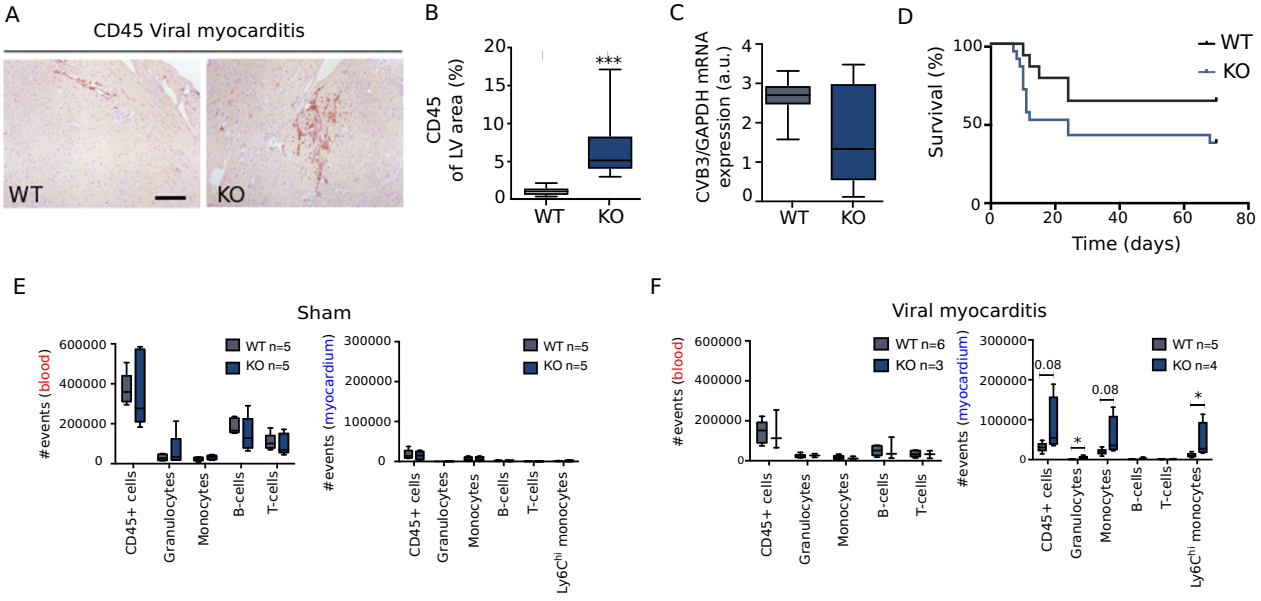

Fig. 1. SPARC is needed to limit cardiac inflammation during viral myocarditis. (A,B) CD45 staining and quantification of left ventricular sections 7 days after CVB3 injection showing increased cardiac leukocytes in SPARC KO hearts (***p = 0.0005 One-way ANOVA, n = 11 and 10 for WT and KO respectively). (C) No difference was found in viral load between both genotypes. (D) Survival of SPARC KO and WT animals during CVB3 infection suggest increased mortality in SPARC KO mice (mortality: 7/12 in SPARC KO versus 4/14 in WT, p = 0.06 using Mantel-Cox method). (E,F) FACS analysis of circulating and cardiac leukocytes (CD45+ cells), granulocytes, monocytes and lymphocyte populations shows no differences between SPARC KO and WT mice in sham animals (E). However, while circulating leukocytes numbers remain unchanged four days after injection with CVB3 between genotypes, the amount of cardiac Ly6C^{hi} monocytes and granulocytes were significantly increased in the SPARC KO mice as compared to WT mice (F, *$p \leq 0.01$, student's t-test). Scale bar: 200 µm.

upregulated upon tissue injury, we contemplated that SPARC may influence cardiac inflammation in viral myocarditis and could therefore potentially be used as a therapeutic strategy limiting heart failure development.

The present study reveals that SPARC regulates inflammation, vascular permeability, and consequently mortality in a murine coxsackievirus B3 (CVB3) induced myocarditis model by regulating the integrity of the endothelial glycocalyx. Above all, this study emphasizes the vital role of the endothelial glycocalyx as part of the extracellular matrix in cardiac (patho-) physiology.

Results

Absence of SPARC increased cardiac inflammation and mortality in viral myocarditis and accelerated the onset of dilated cardiomyopathy

As a first step in investigating the role of SPARC during cardiac inflammation, we subjected SPARC KO and WT mice to CVB3-induced viral myocarditis. Virus-mediated cardiomyocyte damage will induce the infiltration of innate leukocytes (macrophages/monocytes and granulocytes), which is followed by

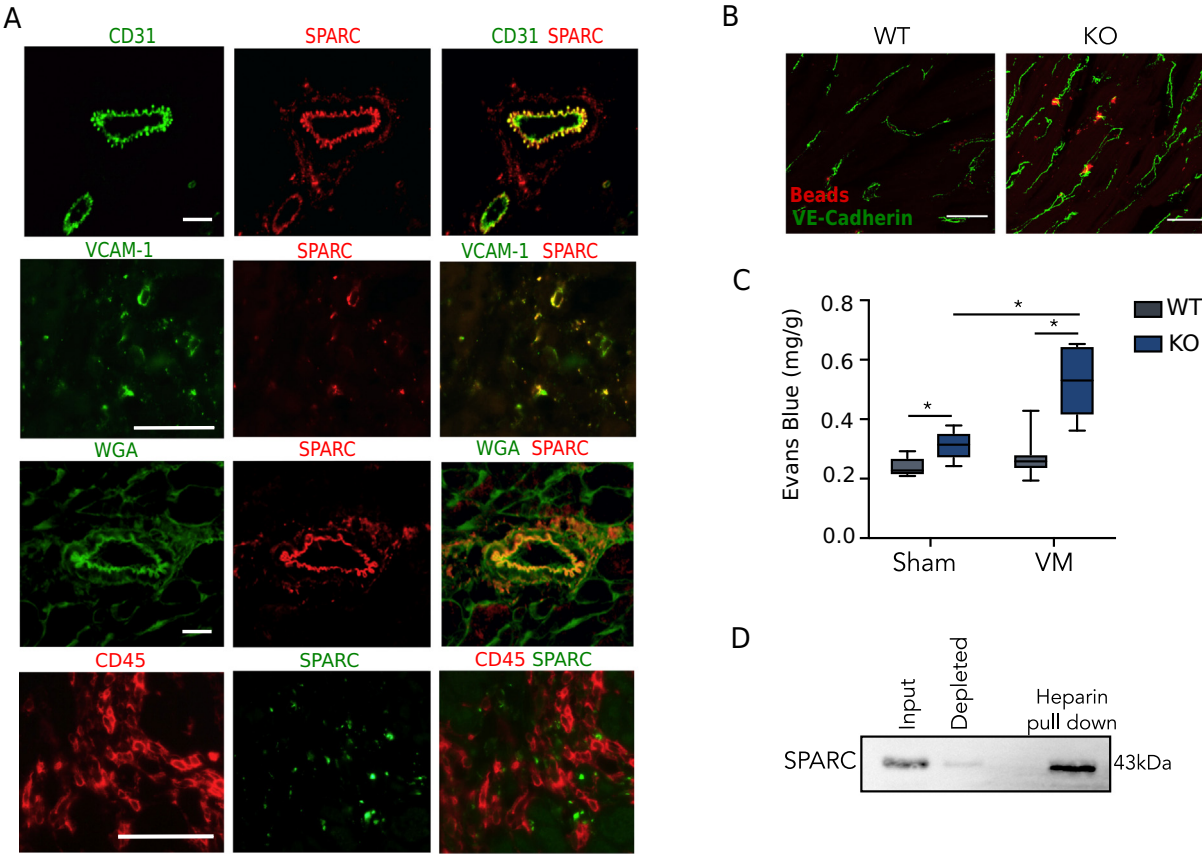

Fig. 2. SPARC is needed to maintain vascular barrier properties. (A) SPARC showed positive staining in blood vessels coinciding Platelet endothelial cell adhesion molecule (PECAM-1) also known as cluster of differentiation 31 (CD31), vascular cell adhesion molecule-1 (VCAM-1) and with Wheat Germ Agglutinin (WGA lectin specific for all sialic acid and *N*-acetylglucosamine that are present on glycoproteins within the extracellular space), but not with CD45+ leukocytes in the heart during viral myocarditis. All images shown are representative, scale bar: 50 μm. (B) Labelled micro-beads were injected and visualized after counterstaining with vascular endothelial cadherin (VE-cadherin) revealing more extravasation in SPARC-KO animals. (Representative picture, red: micro-beads, green: VE-cadherin, scale = 20 μm, $n = 3$ per group) (C) Systemic injection of Evans Blue resulted in significantly more uptake of Evans Blue in the myocardium of SPARC KO sham animals compared to WT sham animals ($n = 8, 6$ for WT and KO respectively, $^*p < 0.005$, Student *t*-test). (D) Pull down of SPARC with protein A/G heparin coated sepharose beads in a cardiac endothelial cell lysate. The input in the first lane represents the total cell lysate. The second lane (depleted) shows the total cell lysate after incubation with the heparin coated sepharose beads. After an empty lane, the fourth lane then represents the pull down with the heparin sepharose beads. (For interpretation of the references to colour in this figure legend, the reader is referred to the web version of this article.)

adaptive leukocytes (B- and T-lymphocytes). We found that significantly more innate and adaptive leukocytes (CD45 positive) infiltrated the heart of SPARC KO mice as compared to WT mice at day 7 (0.7 ± 0.2% vs 6.8 ± 1.8% positive staining of total left ventricular area for WT and KO respectively; $p < 0.005$ (Fig. 1A–B)). Furthermore, absence of SPARC led to increased mortality (9/21, 43% in KO vs. 11/14, 72% in WT at 7 days; $p = 0.06$) (Fig. 1C). The viral exposure did not differ as cardiac viral presence was similar in SPARC KO as compared to WT mice during peak viremia (day 2) (Fig. 1C). While CVB3 injures cardiomyocytes, tissue destruction can be potentiated by the recognition of this virus by pattern recognition receptors of the innate and adaptive immune system, resulting in the production of inflammatory cytokines. Therefore, we measured the expression of viral pattern recognition receptors Toll-Like-Receptor 3 (TLR3), melanoma differentiation association protein-5 (MDA-5) and retinoic acid inducible gene-1 (RIG-1) and found no difference between both groups (Supplemental Fig. 1A–C).

Next, we investigated whether absence of SPARC would affect the recruitment of innate and/or adaptive leukocytes to the injured myocardium. The number of leukocytes either in the circulation or in cardiac tissue under normal conditions did not significantly differ between SPARC WT and KO mice before CVB3 infection as revealed by flow cytometry (Fig. 1E). However, as a consequence of viral infection, a rapid recruitment of innate immune cells into the hearts of SPARC KO mice was observed (83,440 ± 35,807 CD45+ cells), significantly higher as compared to that of non-infected KO mice (14,897 ± 4600 CD45+ cells) and infected WT mice (30,995 ± 5542 CD45+ cells, Fig. 1F). Analysis was done at 4 days post CVB3 infection as there is onset of inflammation but no mortality is yet observed in particular in the KO animals. Of note, the absolute number of Ly6C^{high} monocytes was significantly higher in the hearts of infected KO mice than WT mice (46,014 ± 22,943 cells versus 11,072 ± 2651 cells), which was also true for the granulocyte cells (4601 ± 2192 and 716 ± 186 cells for KO and WT respectively, $^{*}p < 0.05$, Fig. 1F).

Aggravated leukocyte recruitment in the absence of SPARC was due to changes in vascular permeability

As we found that lack of SPARC clearly resulted in excessive immune infiltration due to viral exposure, we wondered whether this would be the consequence of SPARC either influencing the vasculature or the leukocytes. SPARC not only co-stained with the endothelium specific proteins CD31 and VCAM-1 in CVB3-infected hearts, it also co-localized with Wheat Germ Agglutinin (WGA), which is a lectin that recognizes sialic acid and *N*-acetylglucosamine that are present on glycoproteins within the extracellular environment (Fig. 2A). SPARC did not co-localize with CD45+ leukocytes indicating that the influence of SPARC on immune cell recruitment during viral myocarditis occurs on the level of the microvasculature (Fig. 2A). The endothelial glycocalyx is largely composed of carbohydrates found on proteoglycans and glycoproteins and regulates vascular permeability. Hence, the endothelial glycocalyx plays a central role in modulating the influx of inflammatory cells under homeostasis as well as pathophysiological conditions [28–30]. To test whether SPARC absence would induce alterations in vascular permeability, two independent analyses were performed. A qualitative analysis of systemically-injected microspheres shows higher amounts of beads in the cardiac environment of KO as compared to WT mice (Fig. 2B). Likewise, a quantitative analysis of Evans blue uptake revealed that KO mice have a more permissive vasculature in the heart as compared to

Fig. 3. SPARC is needed for an intact endothelial glycocalyx hence impairs leukocyte recruitment. (A) Representative image illustrating the experimental setup of the Cremaster experiments, adjusted images provided by the university of Rochester. (B) Overview (right) and magnified (left) images of the microvasculature of the cremaster muscle illustrating Texas Red-labelled Dextran40 (40 kDa) in the vasculature and its leakage in SPARC WT and KO mice untreated (control) and in response to TNF-α stimulation. (C) The microvascular leakage of Texas red labelled Dextran40 was significantly higher in SPARC KO as compared to WT mice ($^{****}p = 0.0001$; Student *t*-test). Scale bar: 50 μm. Measurements were performed in 25 and 26 vessels from WT and KO mice respectively. (D) Electron microscopic imaging of cardiac capillaries and arterioles demonstrating compromised endothelial glycocalyx in heart sections of SPARC KO mice (scale bar: 500 nm). (lu: Lumen, gly: glycocalyx, ec: endothelial cell). In vitro adhesive properties of leukocytes were no different under static or (E) flow conditions between WT and KO ($n = 3$ per group for flow, $n = 5$ per group for static). (G) Intra-vital microscopy of the cremaster muscle enabled the recording of leukocyte-endothelium interactions in SPARC WT and KO microvessels at baseline and after stimulation with TNFα. (H) Adhesion efficacy, calculated by dividing the number of adherent leukocytes by total rolling leukocytes, was significantly higher in SPARC KO animals compared to WT. (I) Concordantly, cumulative frequency distribution of leukocyte velocities showed significant increased leukocyte velocities in WT animals both before and after TNFα stimulation (One-way ANOVA, KO vs WT $^{*}p < 0.001$; WT vs WT + TNFα $\#p < 0.001$; KO vs KO + TNFα $\#\#p < 0.001$; WT + TNFα vs KO + TNFα $^{**}p < 0.001$). Measurements were performed in >5 mice per group and 5 vessels per mouse, with ≥15 leukocyte velocities quantified per vessel.

WT mice (Fig. 2C). During CVB3 infection this was even more pronounced in the heart, and also true for the lungs and liver (Fig. 2C). Finally, SPARC was detected in a pull down of cardiac endothelial cells using heparin-sepharose beads (Fig. 2D), suggesting an interaction between SPARC and heparan sulphates, one of the major glycocalyx components [37,38].

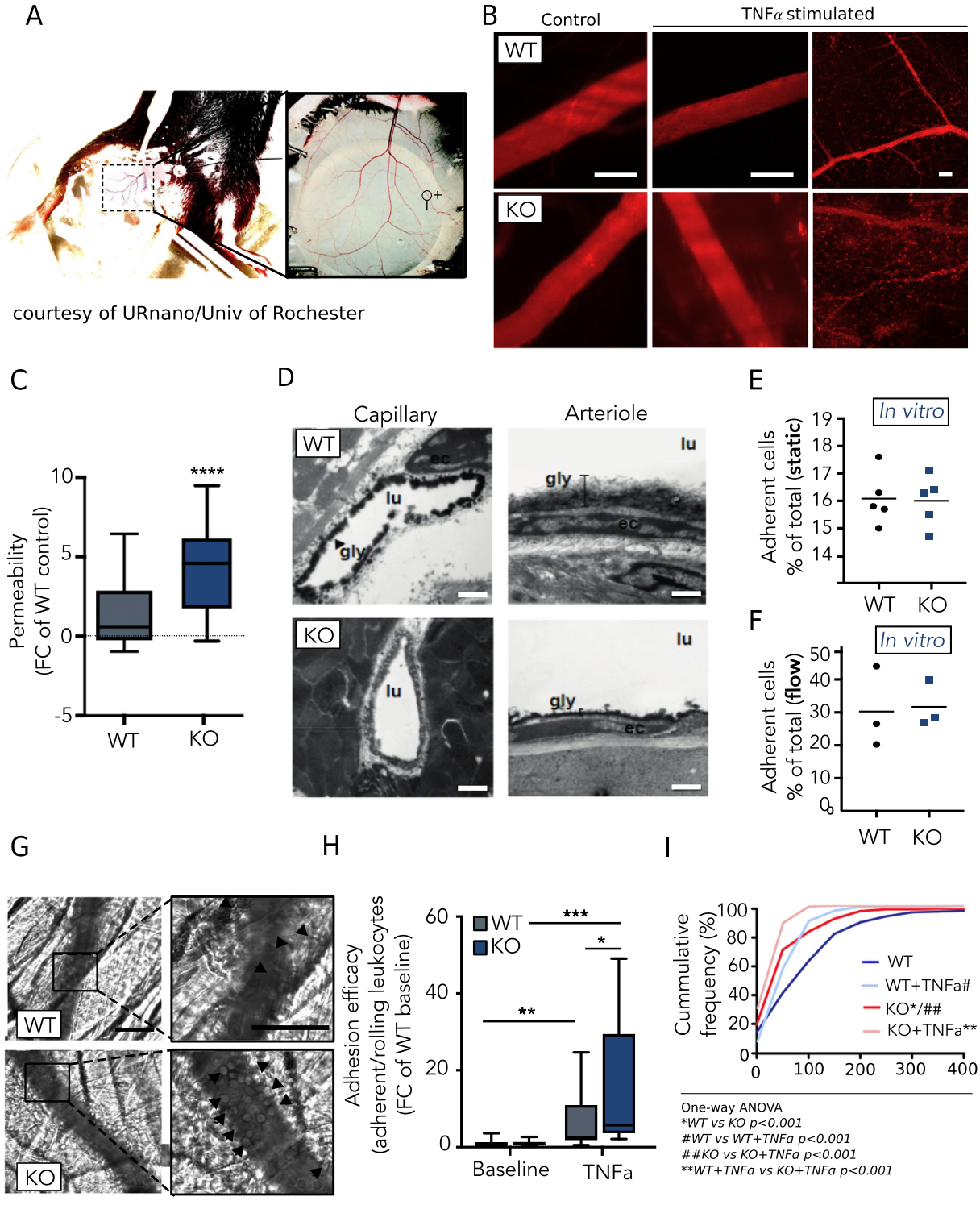

Fig. 3 (*legend on previous page*)

SPARC absence leads to altered vascular permeability and leukocyte-endothelium interactions by impeding glycocalyx integrity

As the endothelial glycocalyx regulates leukocyte recruitment [31], the influence of SPARC on leukocyte recruitment by modulating the structure lining the endothelium was assessed by intra-vital microscopy in the cremaster muscle (Fig. 3A). This allows the visualization of the microvessels and can be used for the assessment of capillary permeability as well as leukocyte adherence, rolling and velocity [32]. The cremaster muscle was consequently stimulated with TNF-α, a pro-inflammatory cytokine central in the pathogenesis of viral myocarditis, which activates the endothelium initiating degradation of the endothelial glycocalyx, enhancing leukocyte adhesion and vascular permeability [33], mimicking disease. Capillary leakiness as a consequence of TNF-α stimulation was significantly higher in SPARC KO as compared to WT mice, as quantified by the extravasation of fluorescently labelled dextran ($p < 0.0001$, Fig. 3B–C).

The malfunctioning endothelial barrier in SPARC KO animals was potentially due to a damaged endothelial glycocalyx, as observed with electron microscopy using a specific protocol to preserve the glycocalyx. SPARC KO mice had a severely thinned or nearly absent glycocalyx in the capillaries and arterioles in the heart, compared to the normal glycocalyx in WT littermates (Fig. 3D). We next wondered whether the decreased immune cell recruitment to the myocardium of SPARC KO mice was endothelial mediated or leukocyte mediated. As no conditional SPARC KO mouse exists, in vitro leukocyte adhesion assay under static conditions and under conditions of flow were performed. Freshly isolated leukocytes from KO and WT mice adhered equally well to TNF-α-stimulated WT cardiac microvascular endothelial cells under both static and flow conditions (Fig. 3E, F). Given the comparable endothelial glycocalyx in these cultured primary endothelial cells [34], this experiment suggested that not leukocyte derived SPARC but endothelial glycocalyx derived SPARC was responsible for the effect on cardiac inflammation. As the endothelial glycocalyx is not only known to influence vascular permeability but also plays a significant role in regulating endothelium-leukocyte interactions [35], we went back to the in vivo cremaster model to investigate leukocyte adhesion and velocity (Fig. 3F). In vivo, lack of SPARC resulted in a significant increase of the adhesion efficacy - seen as the percentage of adhering cells over total rolling cells [36] – with an 8.6-fold increase in SPARC KO mice versus a 4-fold increase in SPARC WT mice after TNF-α stimulation ($p < 0.05$, Fig. 3G, H). In agreement, leukocyte velocities were also significantly reduced in SPARC KO mice as compared to WT, both at baseline (*$p < 0.001$, Fig. 3I) and further reduced after TNF-α stimulation (#/##/**$p < 0.001$, Fig. 3I).

Administration of recombinant SPARC restored the function of damaged glycocalyx

To show that SPARC's effect on the glycocalyx was responsible for the observed increased inflammatory response, we tested whether glycocalyx damage alone could phenocopy the SPARC KO mice. Treatment of WT mice with hyaluronidase (HAase) without consecutive CVB3 injection resulted in a severely damaged endothelial glycocalyx as revealed via electron microscopy revealed, that could be partially restored by a single injection of recombinant SPARC (Fig. 4A). To see whether HAase impeded glycocalyx-associated endothelial barrier properties, and whether these could be restored by recombinant SPARC administration, we again went back to the cremaster model. Degradation of the glycocalyx by injection of HAase resulted in the expected increase in vascular leakiness ($p > 0.0005$, Fig. 4B–C) and reduction of leukocyte velocities ($p < 0.001$, Fig. 4D). Above all, leukocyte velocities and microvascular leakiness were restored back to baseline values in response to recombinant SPARC administration that followed enzymatic degradation of the endothelial surface layer (Fig. 4B–D). Finally, we wondered whether lack of glycocalyx by HAase treatment prior to CVB3 infection could phenocopy SPARC KO mice. As anticipated, HAase treatment significantly increased the cardiac infiltration 7 days after viral infection (4 ± 1% in nontreated –HAase vs. 9 ± 2% in treated +HAase; $p < 0.05$, Fig. 4E–F) without affecting mortality. Similarly to when SPARC is absent, HAase treatment did not affect the viral levels during the viremic phase (Fig. 4G).

Administration of recombinant SPARC reduced cardiac inflammation and mortality in SPARC KO mice

In order to explore the long-term effect of SPARC loss on cardiac function after viral myocarditis, SPARC KO and WT mice underwent echocardiographic assessments at 4 days and 9 weeks after viral infection. Concomitantly a group of KO and WT mice received SPARC systemically for 5 weeks and also underwent echocardiographic evaluation (Table 1). Interestingly, dilated cardiomyopathy started to present only in the KO mice at 9 weeks post viral exposure ($p = 0.02$ and $p = 0.04$, for fractional shortening FS and left ventricular systolic dimension respectively, Table 1). This functional deterioration observed in SPARC null mice could unfortunately not be prevented by systemic SPARC administration. However, SPARC administration did significantly improve the survival of KO mice (14/15,

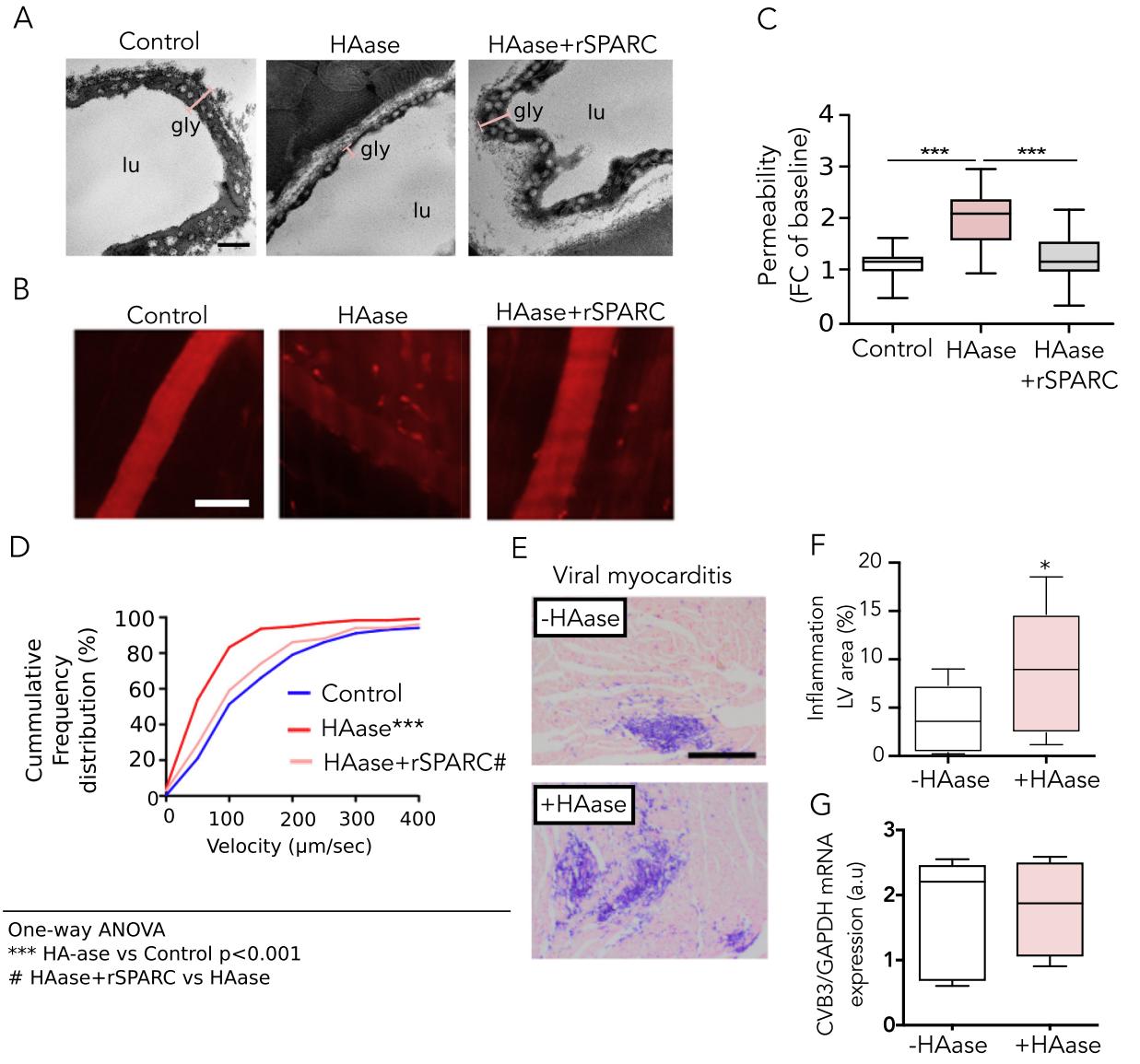

Fig. 4. Glycocalyx integrity is vital for limiting adverse inflammation. (A) Electron microscopic imaging of microvessels showed clear glycocalyx degradation upon treatment with hyaluronidase (HAase). Recombinant SPARC treatment after glycocalyx degradation restored glycocalyx integrity. Scale bar: 200 nm. (B–C) Representative images and quantification of vascular leakiness. After degradation of hyaluronan (one of the major components of the endothelial glycocalyx) with HAase the leakiness of Texas red labelled Dextran40 (40 kDa) increased, which could be restored by treatment with recombinant SPARC (***$p < 0.005$; One-way ANOVA; scale bar: 50 µm). Measurements were performed in 25, 23 and 30 vessels from control, HAase and HAase + rSPARC treated animals respectively. (D) Significantly reduced leukocyte velocities were found in mice injected with HAase, which again could be reversed by administration of recombinant SPARC (Control vs HAase ***$p = 0.0001$, HAase vs HAase + SPARC #$p = 0.01$). (E) Representative images and quantification (F) of leukocyte (CD45+ cell) staining of left ventricular myocardial sections showing an increase in leukocyte infiltration in HAase treated mice compared to nontreated animals (*$p < 0.05$, Student *t*-test; $N = 10$, 8 for –HAase and +HAase treatment respectively). Scale bar: 200 µm. (G) Prior to myocardial immune cell infiltration we did not find a difference in viral presence in the myocardium of HAase treaded versus nontreated mice ($n = 4$).

$p = 0.009$, Fig. 5B–C) without having any benefit on survival in their WT littermates. The improved survival as a result of recombinant SPARC administration in SPARC null mice, was reflected by the decrease in cardiac inflammation ($p < 0.05$, Fig. 5D–E). In trying to identify a possible mortality cause for these mice we hypothesised that aggravated cardiac inflammation might lead to electrophysiological disturbances. Electrocardiographic measurements were performed on SPARC WT mice, SPARC KO mice either treated or

Table 1
. Cardiac function and mortality in SPARC WT and KO animals during viral myocarditis.

Time point	Day 4			
	WT	KO	WT + S	KO + S
Survival (%)	14/14100%	21/21100%	12/12100%	15/15100%
LVIDd (mm)	3.7 ± 0.5	3.7 ± 0.3	3.6 ± 0.2	3.5 ± 0.2
LVIDs (mm)	2.7 ± 0.5	2.4 ± 0.3	2.5 ± 0.4	2.3 ± 0.3
FS (%)	27.5 ± 6.4	34.9 ± 4.9*	30.4 ± 10.2	34.7 ± 8.0
HR (bpm)	538 ± 36	495 ± 40	542 ± 47	503 ± 54

LVIDd Left ventricular internal diameter end diastole; LVIDs Left ventricular internal diameter end systole; FS Fractional Shortening; HR Heart Rate
+S refers to treatment with recombinant SPARC
*WT vs KO $p < 0.05$

Time point	Week 9			
	WT	KO	WT + S	KO + S
Survival (%)	11/14 78.6%	9/21 42.9%	9/12 75.0%	14/15 93.3%
LVIDd (mm)	3.9 ± 0.5	3.8 ± 0.3	3.7 ± 0.3	3.8 ± 0.4
LVIDs (mm)	2.7 ± 0.6	2.8 ± 0.5#	2.7 ± 0.4	2.7 ± 0.4
FS (%)	30.3 ± 9.5	25.8 ± 7.1#	29.3 ± 7.7	29.7 ± 6.8
HR (bpm)	475 ± 103	428 ± 48	552 ± 51.8	432 ± 22.4

#KO day 4 vs KO week 9 $p < 0.05$.

non-treated with recombinant SPARC. Unexpectedly, while there were no significant differences in heart rates between all animals, QTc times were reduced in SPARC KO mice compared to WT yet could not be restored upon recombinant SPARC administration (**$p < 0.05$, Fig. 5F,G).

Discussion

Viral myocarditis is a clinical entity that is still very difficult to diagnose let alone treat. Not only does it result in sudden cardiac arrest it can eventually lead to heart failure development. As the ECM is a vital player regulating cardiac remodelling, we studied the glycoprotein SPARC and showed that its absence enhanced cardiac inflammation and mortality in the CVB3 induced murine model of viral myocarditis. Knowing the importance of the endothelium in recruiting leukocytes and the clear immunohistochemical localization of SPARC on the endothelium, our interest was drawn to the endothelial glycocalyx. Whilst the endothelial glycocalyx is comprised of similar building blocks found in the ECM and is known for regulating leukocyte recruitment and vascular permeability, we show for the first time that extracellular matrix protein SPARC is an essential regulator of microvascular barrier function. Lack of SPARC results in a loss of glycocalyx integrity and consecutive barrier function as leukocyte adhesion and vascular permeability increase when the endothelial glycocalyx is compromised, either by lack of SPARC or by enzymatic degradation of one of its major components (hyaluronan). These alterations in glycocalyx integrity result in increased cardiac inflammation and mortality during viral myocarditis. Most importantly, administration of recombinant SPARC was able to reverse the adverse effects of the glycocalyx damage, and restore the associated glycocalyx functional impairment resulting in reduced vascular leakage.

The composition of the glycocalyx is controlled by multiple factors and requires a timely balance between synthesis and degradation. Though little is known about the regulation of the glycocalyx, there is growing appreciation of its importance in organ homeostasis and disease. Numerous studies show that changes in shear stress, hypoxia, hyperglycemia, oxidized LDL or inflammation can induce glycocalyx perturbation and hence contribute to the vascular dysfunction observed in sepsis [39], acute respiratory syndrome [40], albuminuria [41], atherosclerosis [42], diabetes [43] and obesity [44]. Changes in myocardial glycocalyx have been observed in cardiac pathologies such as ischemia-reperfusion injury [45], excessive oedema [46] and cardiogenic shock [47]. Furthermore, a review about the cardiovascular manifestations of dengue fever, suggested that alterations in glycocalyx might contribute to the capillary leakiness observed during infection and contribute to the myocarditis observed [48]. However this study is the first to implicate glycocalyx perturbations to the pathophysiology of viral myocarditis.

Whilst the need to have SPARC for proper endothelial glycocalyx composition has not been identified before, in vitro studies have shown that SPARC can bind to albumin [49], which itself can

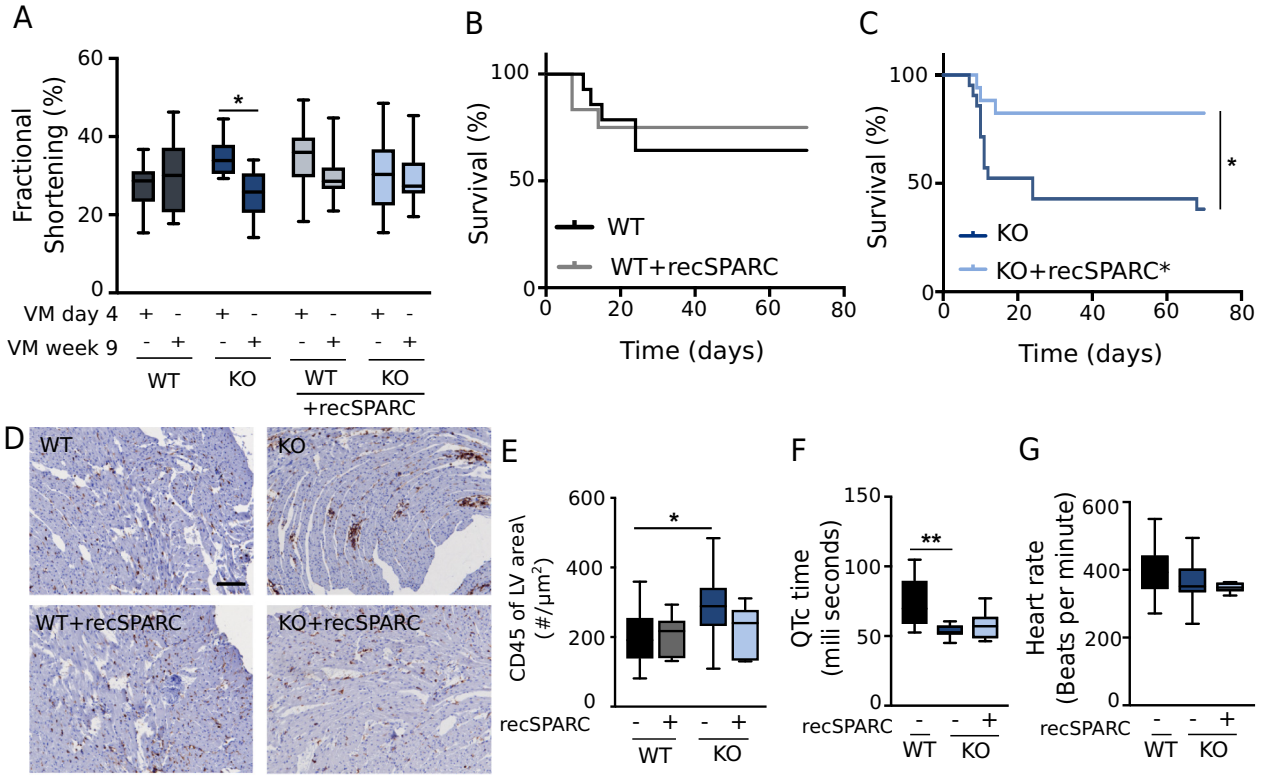

Fig. 5. Recombinant SPARC administration reduces mortality and alleviates heart failure development. (A) Cardiac function significantly deteriorated in SPARC KO mice 9 weeks after viral exposure as compared to WT (*$p < 0.05$). Administration of recombinant SPARC seemed to improve cardiac function in viral myocarditis. (B,C) Survival curve showing that administration of recombinant SPARC reduces the mortality in SPARC KO mice in response to viral exposure. (*$p < 0.01$ using Mantel-Cox method, $N = 14$, 12, 15 and 17 in WT, WT + rSPARC, KO and KO + rSPARC) (D,E) Recombinant SPARC administrated blunted the increased infiltration of immune cells in SPARC KO mice 7 days after CVB3 administration. ($p < 0.05$; One-way ANOVA) (F,G) Lack of SPARC reduced the QTc time on electrocardiographic measurements significantly in KO mice compared to WT while not affecting the heart rate. (**$p < 0.01$; One-way ANOVA). Fractional shortening and inflammation were measured in 11, 9, 9 and 14 WT, WT + rSPARC, KO and KO + rSPARC animals respectively. Scale bar: 50 µm.

regulate glycocalyx integrity [41]. The immunomodulatory role of SPARC in previous studies using in vitro experiments, was ascribed to leukocyte-derived SPARC facilitating leukocyte transmigration across an endothelial monolayer [50], and to endothelial cytoskeleton rearrangements induced by SPARC treatment [51]. However, the role of SPARC on inflammation has been bi-directional in current literature as few studies elude to either a pro- or anti-inflammatory effect of SPARC. In a murine-model for pulmonary fibrosis SPARC is identified as anti-inflammatory [52], whereas it clearly enhances leukocyte recruitment in a murine peritonitis model [53]. The mechanism whereby SPARC affects inflammation in these models by either influencing TGFβ activity or interacting with VCAM-1 [54], fail to comprehensively explain these contradictory findings. Here, the importance of SPARC in endothelial glycocalyx composition and function may clarify its bi-directional role on inflammation. Indeed, differential presence of SPARC in the endothelial surface layer of different vascular beds may explain the seemingly opposing effect SPARC has on inflammation in different tissues and disease models. Although it is well established that every vascular bed has very unique structural and functional characteristics [55,56], whether these unique endothelial characteristics will lead to specific and distinctive glycocalyx composition has unfortunately not been demonstrated yet, mainly due to technical limitations. Nevertheless, we do know that the endothelial glycocalyx consist of numerous complex soluble and insoluble glycoproteins, proteoglycans and glycosaminoglycan's mostly produced by the endothelial cells. Further, the thickness of this structure can vary enormously [14] throughout the vasculature. We therefore strongly believe that glycocalyx composition can differ between various vascular beds as a consequence of unique structural and functional characteristics of the endothelium; hence differential

SPARC presence in the glycocalyx could affect inflammation differently in different tissues and in different diseases, also explaining the opposing effect found using in vitro models.

Glycoproteins have been suggested as important "backbone" molecules for the glycocalyx structure [14]. It is possible that the reduced endothelial barrier properties in SPARC KO mice are a consequence of a lack of proper glycocalyx anchoring rather than an impaired glycocalyx synthesis. Interestingly, there have been studies showing successful restoration of the shedded endothelial glycocalyx after administration of heparan sulphate, one of the major components of the glycocalyx in vitro [57]. Considering our heparan sulphate pull down showed a clear binding of SPARC to this prevalent glycosaminoglycan, and the clear improvement of endothelial barrier properties after administration of recombinant SPARC, we considered the possible importance of SPARC-heparan sulphate interaction in glycocalyx regeneration as proposed by Ebong et al. [57]. However, the exact mechanism via which SPARC affects the glycocalyx needs to be further elaborated.

During myocarditis, systemic SPARC administration rescued KO mice survival though it did not affect the amount of myocyte cell injury as measured by troponin levels at day 7 post viral exposure (Supplementary Fig. 1D). Furthermore, inflammatory dilated cardiomyopathy develops progressively over time in CVB3 induced viral myocarditis in mice and is prevalent as a consequence of cardiomyocyte loss and adverse cardiac inflammation [58]. Similarly to the clinical scenario, dilated cardiomyopathy was not present in all CVB3 infected mice at 9 weeks. However, we did observe dilated cardiomyopathy mainly in KO mice and less in WT mice. Moreover, administration of recombinant SPARC improved cardiac function in SPARC KO mice. These data are in line with other studies showing that limiting the cardiac infiltration during the acute phase improves the long-term function [59].

Where administration of recombinant SPARC clearly improved glycocalyx integrity and consecutive inflammation and mortality, the exact cause of death in SPARC KO mice still remains elusive. Electrocardiographic analysis did reveal a shortening of the QTc time in SPARC KO mice as compared to WT, which has been correlated with increased mortality as a consequence of cardiac arrhythmias [60]. Interestingly, it has been suggested that glycosylated proteins comprising the endothelial glycocalyx are vital mechanosensors that initiate the production of nitric oxide (NO) resulting in coronary artery dilation and suppression of platelet aggregation [61–65]. As coronary flow can be reduced in myocarditis mimicking acute coronary syndrome [66], lack of proper mechanosensing may therefore contribute to the functional deterioration and, combined with increasing inflammation, eventual lead to arrhythmias and death in SPARC KO mice. However, the present study concentrated on the effects of SPARC at the level of endothelial glycocalyx and can thus not rule out potential additive/negative effects of SPARC at the level of the single cardiac myocyte.

Collectively, our data identify SPARC as crucial component of the endothelial barrier and thus prevents pathological cardiac inflammation and mortality. SPARC may therefore represent a novel therapeutic tool to repair or maintain endothelial barrier integrity in cardiac disease.

Material and methods

Animals

C57Bl6/J male *SPARC*-KO (backcrossed 10 times) and WT C57Bl6/J mice (Harlan, the Netherlands) between 10 and 18 weeks of age were used. Mice were maintained in specific pathogen-free facilities at Maastricht or Leuven University. The Animal Care and Use Committee of the University of Maastricht and Leuven approved all described study protocols, according to the Dutch (2012/031) and Belgian law (067/2008, 043/2013) and all animal procedures were performed conform to the guidelines from Directive 2010/63/EU of the European Parliament.

Murine CVB3 induced viral myocarditis model

Eight to 12-week old inbred C57Bl6/J *SPARC*-KO and WT mice were inoculated intra-peritoneal (i.p.) with 1×10^7 cell culture 50% infective dose ($CCID_{50}$) of CVB3 (Nancy Strain) and cardiac immune cell infiltration was measured 7 days later. For long-term administration (5 weeks) mice received SPARC via osmotic minipump. Troponin was measured using a high sensitivity ELISA 7 days after viral exposure (Roche Diagnostics). Mice received hyaluronidase (iv 70 U) [67] 1 h prior to CVB3. All animals were anesthetized with an intra-peritoneal injection of xylazine (10 mg/kg) and ketamine (100 mg/kg) and sacrificed by cervical dislocation. Male mice were used for all experiments except for the long-term 9-weeks viral myocarditis experiment where both Female WT and KO mice were included in equal numbers.

Mouse cremaster preparation and intravital microscopy

Mice were anesthetized and the exposed muscle was positioned on a clear Silicon pedestal and longitudinally incised from the apex to the inguinal canal with minimal disruption of the vascular supply. The stage of the intravital microscope (Olympus BHM) was coupled to a cooled intensified CCD video

camera (GenIV ICCD, Princeton Instruments). Cremaster muscle capillaries were examined with a water immersion objective lens (Olympus; LUMPlanFL, NA 0.9). The muscle was continuously (5 ml/min) superfused at 37 °C with a bicarbonate-buffered physiological salt solution (PSS). Texas Red labelled 40 kDa dextrans (Dex-40; Invitrogen) were intravenously injected at 10 mg/ml in PBS. Cremaster capillaries of 30–50 µm were chosen for examination from different microscopic field, and recorded on videotape using trans and epi-illumination. After baseline recordings were made (15–20 min) TNF-α (2 ng/ml; Peprotech) was dropped on the Cremaster muscle for 5 min. Recordings of the same capillaries were made at baseline, after 60 and 120 min. 0.1 ml recombinant SPARC (15 µg/kg, R and D systems) was injected i.v. at a concentration of 0,15 mg/kg prior to TNF-α stimulation. 0.1 ml (35 U) of hyaluronidase was injected after the equilibration period and SPARC was injected 10 min after the injection of hyaluronidase. Rolling leukocytes were measured by counting the visible passing leukocytes for 60 s. Counting cells that adhered to the vessel wall for ≥30 s and did not move more than their own diameter in distance across the vessel wall during this period qualified as adherent leukocytes. Adhesion efficacy could be calculated by dividing the number of adherent leukocytes by the total number of rolling leukocytes. Leukocyte velocities were determined by measuring the time it took individual cells to travel 150 µm in distance. Only cells that were visible during the entire course were include. Hokawo 2.5 Wasabi Software and Image J 1.48v were used for post-hoc data analysis.

Cardiac fractionation and flow cytometry

Peripheral blood and the cardiac immune cell fractions were analyzed using a CantoII flow cytometer (Becton Dickenson (BD), San Diego, CA). Cells were first incubated with anti-CD16/32 (eBioscience, San Diego, CA, #14-0161-85,1:100) to block Fc receptor binding. CD45+ leukocytes subpopulations were identified (Biolegend, #103129, 1:100) and defined as follows: T lymphocytes (CD3+,eBioscience, # 57-0033-80,1:100), B lymphocytes (B220+,BD # 561226, 1:50), Granulocytes (CD11b+, BD# 552850 1:2000, Ly6G+, BD# 560600, 1:100), Monocytes (CD11b+, F4/80-, Biolegend #123116, 1:100, Ly6C+, Miltenyi # 130-093-134, 1:20). Absolute counts for cardiac and blood samples were determined with BD Truecount™ tubes according to the manufacturer's instructions.

Adhesion assay

Mouse endothelial cells (SVEC, simian virus 40-transformed mouse microvascular endothelial cells) were seeded on µ-slide VI$^{0.4}$ (Ibidi, Planegg, Germany) and then stimulated with 10 ng/ml TNF-α for 24 h. 700 µL of blood was isolate from either wild-type or knockout mice as indicated. The red blood cells were lysed to produce a mixed leukocyte population and stained with the intracellular fluorescent cell label carboxyfluorescein N-hydroxysuccinimidyl ester (or CFSE). Endothelial cells were then exposed to these leukocytes under flow. To that end, the white blood cells from one mouse were added to at a concentration of 10^6/mL. The flow rate was set to produce 1.25 dyne/cm^2. Endothelial cells were exposed to white blood cells to flow for a period of 4 h. The system was flushed with PBS, and then the slides were transferred to a confocal microscope. Three images at random locations, chosen based on the transmitted light, were taken of the fluorescently labelled white blood cells. The average number of adhered cells per unit area was calculated.

Static adhesion assays where performed as follows: Spleens of SPARC WT and KO mice were removed and mashed over a 40 µm mesh. Cell suspensions were then incubated with CD45+ beads (Miltenyi Biotech, Germany) according to the manufacturer's instructions in order to isolate the monocytes. Isolated cells were labelled with CFSE (Molecular Probes, Invitrogen) and then placed on top of TNF-α (10 ng/ml) stimulated mouse endothelial cells (SVEC, simian virus 40-transformed mouse microvascular endothelial cells) and allowed to adhere for 2 h at 37 °C. Non-adherent cells were washed off and the remaining adhered cells quantified with a Victor 2 microplate reader (Perkin-Elmer, USA).

Staining and Immunohistochemistry

4 µm thick sections were stained with CD45 (BD Pharmingen, catalog no. 553076, 1:100) for determining the amount of inflammation. Immunofluorescence of paraffin sections was performed according to protocol using antibodies against CD45 (BD Pharmingen, catalog no. 553076, 1:100), CD31 (BD Pharmingen, catalog no. 557355, 1:500), VCAM-1 (BD Pharmingen, catalog no. 553330, 1:50) and SPARC (R&D, catalog no. AF942, 1:100). Images were acquired using Leica Qwin image processing software (Leica, Germany).

Electron microscopy

Hearts were fixed by perfusing 5-10 ml of Glutaraldehyde 2,5%, Saccharose 12%, Na-cacodylate 3 H2O 0,4 M pH 7,3, lanthanum 4% pH 7,4 after which they were sectioned into small cubes that were fixed for another 2 h. Samples were dehydrated in graded series of ethanol and embedded in Araldite (CY-212; Serva). Ultrathin sections were counterstained with uranium acetate and lead citrate prior to examination in a Philips CM100 electron microscope.

Real time PCR

Real-time reverse transcriptase–polymerase chain reaction (RT-PCR) analysis was performed (Bio-Rad, Maastricht, Netherlands) to determine transcript with the following primers; U6 (FWD CGC-TTC-GGC-AGC-ACA-TAT-AC, BWD TTC-ACG-AAT-TTG-CGT-GTC-AT), MDA5 (FWD GCC-TGG-AAC-GTA-GAC-GAC-AT, BWD TTG-GGC-CAC-TTC-CAT-TTG-GT), RIG-1 (FWD AGA-CGG-TTC-ACC-GCA-TAC-AG, BWD AAG-CGT-CTC-CAA-GGA-CAG-TG), CVB3 (FWD ACG-AAT-CCC-AGT-GTG-TTT-TGG, BWD TGC-TCA-AAA-ACG-GTA-TGG-ACA-T), TLR3 (FWD AGC-ATC-AAA-AGA-AGC-CGA-AA, BWD CTT-GCT-GAA-CTG-CGT-GAT-GT). Data were acquired and analyzed IQ5 software (Bio-Rad, Maastricht, Netherlands).

Vascular permeability assay

Vascular permeability experiments with Evans Blue dye were performed in heart, lung, liver, spleen and skin as previously described [68,69]. Bead extravasation was done as follows; a 1:10 dilution of red fluorescent microbeads (Invitrogen, Fluospheres) was tail vein injected. The beads were allowed to circulate for 2 min, before intracardiac perfusion of 1% PFA for 15 min. Heart were then dissected, further fixed for 1 h in 1% PFA, cryo-embedded, sectioned and then immunostained for VE-Cadherin (R&D Systems). Sections were imaged using z-sectioning on a confocal Zeiss LSM700.

Echocardiographic and ECG recordings

Animals were anesthetized and placed in a supine position on a heating pad to keep the internal body temperature between 37.5 and 37.7 °C by using a rectal probe. Standard views were obtained in 2-D as well as M-mode by transthoracic echocardiography using a 12 MHz probe (Hewlett Packard, Amsterdam, the Netherlands) on a Visual Sonics echocardiograph. ECG signals were measured in SPARC KO and WT mice and QTc times were assessed for individual heartbeats.

Statistical analysis

Results represent the mean ± SEM unless indicated otherwise. For murine studies, D'Agostino and Pearson's omnibus normality test was performed. Statistical significance was determined by unpaired Student's *t*-test or ANOVA when data were normally distributed. Wilcoxon, Mann-Whitney or Kruskal-Wallis test was used for non-parametric data as indicated. Gehan-Breslow-Wilcoxon or Mantel-Cox test was used for survival analysis. Statistical analyses were performed with Prism GraphPad software v5.0.

Supplementary data to this article can be found online at https://doi.org/10.1016/j.matbio.2018.04.015.

Acknowledgements & funding

This work was supported by the European Commission grant N° 602904 (FIBROTARGETS), N° 261409 (MEDIA), the NWO Vidi (91796338) and the CVON 2011 (CVON2011-11) (ARENA).

Conflict of interest

The authors have nothing to disclose.

Received 8 February 2018;
Received in revised form 29 April 2018;
Accepted 30 April 2018
Available online 3 May 2018

Keywords:
SPARC;
Endothelial glycocalyx;
Viral myocarditis;
Extracellular matrix;
Inflammation

†Contributed equally.

References

[1] H.T. Aretz, M.E. Billingham, W.D. Edwards, S.M. Factor, J.T. Fallon, J.J. Fenoglio Jr., E.G. Olsen, F.J. Schoen, Myocarditis. A histopathologic definition and classification, Am J Cardiovasc Pathol 1 (1) (1987) 3–14.
[2] S. Sakakibara, S. Konno, Endomyocardial biopsy, Jpn. Heart J. 3 (1962) 537–543.
[5] E. Funseth, U. Lindh, L. Wesslen, G. Friman, N.G. Ilback, Trace element changes in the myocardium during coxsackievirus B3 myocarditis in the mouse, Biol. Trace Elem. Res. 76 (2) (2000) 149–160.
[6] S. Sagar, P.P. Liu, L.T. Cooper Jr., Myocarditis, Lancet 379 (9817) (2012) 738–747.
[7] M.J. Sole, P. Liu, Viral myocarditis: a paradigm for understanding the pathogenesis and treatment of dilated cardiomyopathy, J. Am. Coll. Cardiol. 22 (4 Suppl A) (1993) 99A–105A.
[8] A. Naba, K.R. Clauser, H. Ding, C.A. Whittaker, S.A. Carr, R. O. Hynes, The extracellular matrix: tools and insights for the "omics" era, Matrix Biol. 49 (2016) 10–24.
[9] J. Barallobre-Barreiro, A. Didangelos, F.A. Schoendube, I. Drozdov, X. Yin, M. Fernandez-Caggiano, P. Willeit, V.O. Puntmann, G. Aldama-Lopez, A.M. Shah, N. Domenech, M. Mayr, Proteomics analysis of cardiac extracellular matrix remodeling in a porcine model of ischemia/reperfusion injury, Circulation 125 (6) (2012) 789–802.

[10] M. Rienks, A.P. Papageorgiou, N.G. Frangogiannis, S. Heymans, Myocardial extracellular matrix: an ever-changing and diverse entity, Circ. Res. 114 (5) (2014) 872–888.
[11] S. Van Linthout, C. Tschope, Inflammation - cause or consequence of heart failure or both? Curr Heart Fail Rep 14 (4) (2017) 251–265.
[12] M. Rienks, A. Papageorgiou, K. Wouters, W. Verhesen, R.V. Leeuwen, P. Carai, G. Summer, D. Westermann, S. Heymans, A novel 72-kDa leukocyte-derived osteoglycin enhances the activation of toll-like receptor 4 and exacerbates cardiac inflammation during viral myocarditis, Cell. Mol. Life Sci. 74 (8) (2017) 1511–1525.
[13] S. Deckx, W. Heggermont, P. Carai, M. Rienks, T. Dresselaers, U. Himmelreich, R. van Leeuwen, W. Lommen, J. van der Velden, A. Gonzalez, J. Diez, A.P. Papageorgiou, S. Heymans, Osteoglycin prevents the development of age-related diastolic dysfunction during pressure overload by reducing cardiac fibrosis and inflammation, Matrix Biol. 66 (2018) 110–124.
[14] S. Reitsma, D.W. Slaaf, H. Vink, M.A. van Zandvoort, M.G. oude Egbrink, The endothelial glycocalyx: composition, functions, and visualization, Pflugers Arch. 454 (3) (2007) 345–359.
[15] X. Zhang, D. Sun, J.W. Song, J. Zullo, M. Lipphardt, L. Coneh-Gould, M.S. Goligorsky, Endothelial cell dysfunction and glycocalyx - a vicious circle, Matrix Biol. (2018) [Epub ahead of print].
[16] M.W. Schellings, D. Vanhoutte, M. Swinnen, J.P. Cleutjens, J. Debets, R.E. van Leeuwen, J. d'Hooge, F. Van de Werf, P. Carmeliet, Y.M. Pinto, E.H. Sage, S. Heymans, Absence of SPARC results in increased cardiac rupture and dysfunction after acute myocardial infarction, J. Exp. Med. 206 (1) (2009) 113–123.
[17] A.D. Bradshaw, C.F. Baicu, T.J. Rentz, A.O. Van Laer, J. Boggs, J.M. Lacy, M.R. Zile, Pressure overload-induced alterations in fibrillar collagen content and myocardial diastolic function: role of secreted protein acidic and rich in cysteine (SPARC) in post-synthetic procollagen processing, Circulation 119 (2) (2009) 269–280.
[18] A.D. Bradshaw, C.F. Baicu, T.J. Rentz, A.O. Van Laer, D.D. Bonnema, M.R. Zile, Age-dependent alterations in fibrillar collagen content and myocardial diastolic function: role of SPARC in post-synthetic procollagen processing, Am. J. Physiol. Heart Circ. Physiol. 298 (2) (2010) H614–22.
[19] A. Francki, A.D. Bradshaw, J.A. Bassuk, C.C. Howe, W.G. Couser, E.H. Sage, SPARC regulates the expression of collagen type I and transforming growth factor-beta1 in mesangial cells, J. Biol. Chem. 274 (45) (1999) 32145–32152.
[20] N. Said, H.F. Frierson, M. Sanchez-Carbayo, R.A. Brekken, D. Theodorescu, Loss of SPARC in bladder cancer enhances carcinogenesis and progression, J. Clin. Invest. 123 (2) (2013) 751–766.
[21] N. Said, H.F. Frierson Jr., D. Chernauskas, M. Conaway, K. Motamed, D. Theodorescu, The role of SPARC in the TRAMP model of prostate carcinogenesis and progression, Oncogene 28 (39) (2009) 3487–3498.
[22] E.M. Rosset, A.D. Bradshaw, SPARC/osteonectin in mineralized tissue, Matrix Biol. 52–54 (2016) 78–87.
[23] M.J. Reed, A.D. Bradshaw, M. Shaw, E. Sadoun, N. Han, N. Ferara, S. Funk, P. Puolakkainen, E.H. Sage, Enhanced angiogenesis characteristic of SPARC-null mice disappears with age, J. Cell. Physiol. 204 (3) (2005) 800–807.
[24] L. Vaughan, R. Marley, S. Miellet, P.S. Hartley, The impact of SPARC on age-related cardiac dysfunction and fibrosis in Drosophila, Exp. Gerontol. (2017) [Epub ahead of print].
[25] L.E. de Castro Bras, H. Toba, C.F. Baicu, M.R. Zile, S.T. Weintraub, M.L. Lindsey, A.D. Bradshaw, Age and SPARC change the extracellular matrix composition of the left ventricle, Biomed. Res. Int. (2014) 810562.
[26] S.A. Arnold, L.B. Rivera, A.F. Miller, J.G. Carbon, S.P. Dineen, Y. Xie, D.H. Castrillon, E.H. Sage, P. Puolakkainen, A.D. Bradshaw, R.A. Brekken, Lack of host SPARC enhances vascular function and tumor spread in an orthotopic murine model of pancreatic carcinoma, Dis. Model. Mech. 3 (1–2) (2010) 57–72.
[27] R.A. Brekken, E.H. Sage, SPARC, a matricellular protein: at the crossroads of cell-matrix communication, Matrix Biol. 19 (8) (2001) 816–827.
[28] S. Weinbaum, J.M. Tarbell, E.R. Damiano, The structure and function of the endothelial glycocalyx layer, Annu. Rev. Biomed. Eng. 9 (2007) 121–167.
[29] H. Kolarova, B. Ambruzova, L. Svihalkova Sindlerova, A. Klinke, L. Kubala, Modulation of endothelial glycocalyx structure under inflammatory conditions, Mediat. Inflamm. 2014 (2014) 694312.
[30] B.F. Becker, D. Chappell, D. Bruegger, T. Annecke, M. Jacob, Therapeutic strategies targeting the endothelial glycocalyx: acute deficits, but great potential, Cardiovasc. Res. 87 (2) (2010) 300–310.
[31] E.P. Schmidt, Y. Yang, W.J. Janssen, A. Gandjeva, M.J. Perez, L. Barthel, R.L. Zemans, J.C. Bowman, D.E. Koyanagi, Z.X. Yunt, L.P. Smith, S.S. Cheng, K.H. Overdier, K.R. Thompson, M.W. Geraci, I.S. Douglas, D.B. Pearse, R.M. Tuder, The pulmonary endothelial glycocalyx regulates neutrophil adhesion and lung injury during experimental sepsis, Nat. Med. 18 (8) (2012) 1217–1223.
[32] P. Bagher, S.S. Segal, The mouse cremaster muscle preparation for intravital imaging of the microcirculation, J. Vis. Exp. (52) (2011).
[33] C.B. Henry, B.R. Duling, TNF-alpha increases entry of macromolecules into luminal endothelial cell glycocalyx, Am. J. Physiol. Heart Circ. Physiol. 279 (6) (2000) H2815–23.
[34] E.E. Ebong, F.P. Macaluso, D.C. Spray, J.M. Tarbell, Imaging the endothelial glycocalyx in vitro by rapid freezing/freeze substitution transmission electron microscopy, Arterioscler. Thromb. Vasc. Biol. 31 (8) (2011) 1908–1915.
[35] U. Schott, C. Solomon, D. Fries, P. Bentzer, The endothelial glycocalyx and its disruption, protection and regeneration: a narrative review, Scand. J. Trauma Resusc. Emerg. Med. 24 (2016) 48.
[36] S.M. Jakob, R. Pick, D. Brechtefeld, C. Nussbaum, F. Kiefer, M. Sperandio, B. Walzog, Hematopoietic progenitor kinase 1 (HPK1) is required for LFA-1-mediated neutrophil recruitment during the acute inflammatory response, Blood 121 (20) (2013) 4184–4194.
[37] N.S. Ihrcke, L.E. Wrenshall, B.J. Lindman, J.L. Platt, Role of heparan sulfate in immune system-blood vessel interactions, Immunol. Today 14 (10) (1993) 500–505.
[38] A.R. Pries, T.W. Secomb, P. Gaehtgens, The endothelial surface layer, Pflugers Arch. 440 (5) (2000) 653–666.
[39] M. Henrich, M. Gruss, M.A. Weigand, Sepsis-induced degradation of endothelial glycocalix, ScientificWorldJournal 10 (2010) 917–923.
[40] D. Mehta, K. Ravindran, W.M. Kuebler, Novel regulators of endothelial barrier function, Am. J. Physiol. Lung Cell. Mol. Physiol. 307 (12) (2014) L924–35.
[41] A.H. Salmon, J.K. Ferguson, J.L. Burford, H. Gevorgyan, D. Nakano, S.J. Harper, D.O. Bates, J. Peti-Peterdi, Loss of the endothelial glycocalyx links albuminuria and vascular dysfunction, J. Am. Soc. Nephrol. 23 (8) (2012) 1339–1350.

[42] A. Koo, C.F. Dewey Jr., G. Garcia-Cardena, Hemodynamic shear stress characteristic of atherosclerosis-resistant regions promotes glycocalyx formation in cultured endothelial cells, Am. J. Physiol. Cell Physiol. 304 (2) (2013) C137–46.
[43] R.M. Perrin, S.J. Harper, D.O. Bates, A role for the endothelial glycocalyx in regulating microvascular permeability in diabetes mellitus, Cell Biochem. Biophys. 49 (2) (2007) 65–72.
[44] B.J. Eskens, T.M. Leurgans, H. Vink, J.W. Vanteeffelen, Early impairment of skeletal muscle endothelial glycocalyx barrier properties in diet-induced obesity in mice, Phys. Rep. 2 (1) (2014), e00194. .
[45] I. Rubio-Gayosso, S.H. Platts, B.R. Duling, Reactive oxygen species mediate modification of glycocalyx during ischemia-reperfusion injury, Am. J. Physiol. Heart Circ. Physiol. 290 (6) (2006) H2247–56.
[46] B.M. van den Berg, H. Vink, J.A. Spaan, The endothelial glycocalyx protects against myocardial edema, Circ. Res. 92 (6) (2003) 592–594.
[47] C. Jung, G. Fuernau, P. Muench, S. Desch, I. Eitel, G. Schuler, V. Adams, H.R. Figulla, H. Thiele, Impairment of the endothelial glycocalyx in cardiogenic shock and its prognostic relevance, Shock 43 (5) (2015) 450–455.
[48] S. Yacoub, H. Wertheim, C.P. Simmons, G. Screaton, B. Wills, Cardiovascular manifestations of the emerging dengue pandemic, Nat. Rev. Cardiol. 11 (6) (2014) 335–345.
[49] J.E. Schnitzer, P. Oh, Antibodies to SPARC inhibit albumin binding to SPARC, gp60, and microvascular endothelium, Am. J. Phys. 263 (6 Pt 2) (1992) H1872–9.
[50] K.A. Kelly, J.R. Allport, A.M. Yu, S. Sinh, E.H. Sage, R.E. Gerszten, R. Weissleder, SPARC is a VCAM-1 counterligand that mediates leukocyte transmigration, J. Leukoc. Biol. 81 (3) (2007) 748–756.
[51] S.E. Goldblum, X. Ding, S.E. Funk, E.H. Sage, SPARC (secreted protein acidic and rich in cysteine) regulates endothelial cell shape and barrier function, Proc. Natl. Acad. Sci. U. S. A. 91 (8) (1994) 3448–3452.
[52] S. Sangaletti, C. Tripodo, B. Cappetti, P. Casalini, C. Chiodoni, S. Piconese, A. Santangelo, M. Parenza, I. Arioli, S. Miotti, M.P. Colombo, SPARC oppositely regulates inflammation and fibrosis in bleomycin-induced lung damage, Am. J. Pathol. 179 (6) (2011) 3000–3010.
[53] K.A. Kelly, J.R. Allport, A.M. Yu, S. Sinh, E.H. Sage, R.E. Gerszten, R. Weissleder, SPARC is a VCAM-1 counterligand that mediates leukocyte transmigration, J. Leukoc. Biol. 81 (3) (2007) 748–756.
[54] J. Trombetta-Esilva, A.D. Bradshaw, The function of SPARC as a mediator of fibrosis, Open Rheumatol. J. 6 (2012) 146–155.
[55] W.C. Aird, Phenotypic heterogeneity of the endothelium: II. Representative vascular beds, Circ. Res. 100 (2) (2007) 174–190.
[56] W.C. Aird, Phenotypic heterogeneity of the endothelium: I. Structure, function, and mechanisms, Circ. Res. 100 (2) (2007) 158–173.
[57] S.A. Mensah, M.J. Cheng, H. Homayoni, B.D. Plouffe, A.J. Coury, E.E. Ebong, Regeneration of glycocalyx by heparan sulfate and sphingosine 1-phosphate restores inter-endothelial communication, PLoS One 12 (10) (2017), e0186116.
[58] P.M. Becher, F. Gotzhein, K. Klingel, F. Escher, S. Blankenberg, D. Westermann, D. Lindner, Cardiac function remains impaired despite reversible cardiac remodeling after acute experimental viral myocarditis, J. Immunol. Res. 2017 (2017), 6590609.
[59] M.F. Corsten, A. Papageorgiou, W. Verhesen, P. Carai, M. Lindow, S. Obad, G. Summer, S.L. Coort, M. Hazebroek, R. van Leeuwen, M.J. Gijbels, E. Wijnands, E.A. Biessen, M.P. De Winther, F.R. Stassen, P. Carmeliet, S. Kauppinen, B. Schroen, S. Heymans, MicroRNA profiling identifies MicroRNA-155 as an adverse mediator of cardiac injury and dysfunction during acute viral myocarditis, Circ. Res. 111 (4) (August 3, 2012).
[60] Y. Zhang, W.S. Post, D. Dalal, E. Blasco-Colmenares, G.F. Tomaselli, E. Guallar, QT-interval duration and mortality rate: results from the Third National Health and Nutrition Examination Survey, Arch. Intern. Med. 171 (19) (2011) 1727–1733.
[61] R. Rubio, G. Ceballos, Role of the endothelial glycocalyx in dromotropic, inotropic, and arrythmogenic effects of coronary flow, Am. J. Physiol. Heart Circ. Physiol. 278 (1) (2000) H106–16.
[62] R. Bhardwaj, C.P. Page, G.R. May, P.K. Moore, Endothelium-derived relaxing factor inhibits platelet aggregation in human whole blood in vitro and in the rat in vivo, Eur. J. Pharmacol. 157 (1) (1988) 83–91.
[63] Y. Zeng, J.M. Tarbell, The adaptive remodeling of endothelial glycocalyx in response to fluid shear stress, PLoS One 9 (1) (2014), e86249.
[64] A.M.W. Bartosch, R. Mathews, J.M. Tarbell, Endothelial Glycocalyx-mediated nitric oxide production in response to selective AFM pulling, Biophys. J. 113 (1) (2017) 101–108.
[65] E.E. Ebong, S.V. Lopez-Quintero, V. Rizzo, D.C. Spray, J.M. Tarbell, Shear-induced endothelial NOS activation and remodeling via heparan sulfate, glypican-1, and syndecan-1, Integr Biol (Camb) 6 (3) (2014) 338–347.
[66] X.Z. Zheng, J. Wu, Q. Zheng, W.Z. Zha, Coronary sinus flow is reduced and recovered with time in viral myocarditis mimicking acute coronary syndrome: a transthoracic Doppler echocardiographic study, J. Ultrasound Med. 35 (1) (2016) 63–69.
[67] D.R. Potter, J. Jiang, E.R. Damiano, The recovery time course of the endothelial cell glycocalyx in vivo and its implications in vitro, Circ. Res. 104 (11) (2009) 1318–1325.
[68] M. Radu, J. Chernoff, An in vivo assay to test blood vessel permeability, J. Vis. Exp. 73 (2013) e50062.
[69] E.G. Perdiguero, A. Galaup, M. Durand, J. Teillon, J. Philippe, D.M. Valenzuela, A.J. Murphy, G.D. Yancopoulos, G. Thurston, S. Germain, Alteration of developmental and pathological retinal angiogenesis in angptl4-deficient mice, J. Biol. Chem. 286 (42) (2011) 36841–36851.